Void Coalescence With and Without Prestrain History

Z. L. Zhang* and B. Skallerud

Department of Structural Engineering, Norwegian University of Science and Technology (NTNU), N-7491 Trondheim, Norway

ABSTRACT: In this study, void coalescence with and without a plastic prestrain history is studied using stress-controlled axisymmetric unit cell models. In addition to spherical voids, both oblate and prolate voids are considered. In the case with prestrain history a uniaxial prestrain up to 10% was applied and the material is thereafter subjected to loadings with constant stress triaxiality. It is found that the microscopic position of the maximum axial stress in void ligament can be taken as an indicator for void coalescence. In the beginning of plastic loading the maximum axial stress occurs at the edge close to the void. With the increase of plastic deformation, the position of maximum axial stress shifts from the void edge to cell boundary and coalescence starts when the position appears at the boundary. It is shown that a prestrain history significantly reduces the void coalescence strain. The prestrain effect on void coalescence depends strongly on the initial void shape. Prestrain history induces both strain hardening and void shape change. The effect of prestrain-induced void shape change on coalescence strain is relatively small while the effect of prestrain-induced local hardening is significant.

KEY WORDS: void growth and coalescence, ductile fracture, Gurson model, prestrain history effect.

INTRODUCTION

THERE ARE MANY engineering scenarios where steel components suffer from plastic deformation due to accidental loading, cold bending, and ground movement, and the effect of the plastic deformation on further deformation and loading capability needs to be assessed (Chae et al., 2000; Sivaprasad et al., 2000; Cosham, 2001; Enami, 2005; Fukuda et al., 2005; Qiu et al., 2005). One of the examples is the so-called pipe reeling process in

---

*Author to whom correspondence should be addressed. E-mail: zhiliang.zhang@ntnu.no
Figures 9–11 appear in color online: http://ijd.sagepub.com

offshore industry. In the reel-lay process the pipe is first reeled onto a drum on a vessel for transportation. During the installation, the pipe is unreeled, straightened and deployed into the sea. During the laying process axial plastic deformations as large as 2% can occur and the pipe section is cyclically plastified. It has been observed that a prestrain history modifies the yielding as well as hardening characteristics in a positive manner (Martinez and Brown, 2005). However, the effect of prestrain on tensile properties and fracture toughness is largely unexplored until recent experimental evidences. An experimental program has been carried out by Fukuda et al. (2005). Pipe steels subjected to a uniaxial prestrain history have been tested using fracture mechanics specimens. For both compressive and tensile prestrain a clear reduction of the critical crack tip opening displacement (CTOD) compared with the virgin steels has been observed. The reduction of fracture toughness may be explained by the ductile damage induced during the prestraining process.

The ductile failure mechanism of engineering steels is most often characterized by void nucleation, growth, and coalescence (Garrison and Moody, 1987). Significant progress has been made in developing constitutive models for plastic materials incorporating void mechanisms. The best-known constitutive model appears to be the one originally developed by Gurson (1975) and later modified by Tvergaard (1981, 1982) and Needleman and Tvergaard (1992). With the introduction of the so-called critical void volume fraction, the Gurson–Tvergaard–Needleman model can consider the effect of void coalescence. However, the model is lamed by the lack of a physical mechanism-based coalescence criterion. Application of the Gurson model as a predictive method using realistic microvoid parameters demands a void coalescence criterion. Void growth is a continuum plastic deformation process and is much better understood than void coalescence. Void coalescence is the last step of ductile fracture. Onset of coalescence corresponds to the instant when a relatively homogenous deformation state suddenly shifts to a highly localized one with uniaxial stretching (Benzerga et al., 2002). Yamamoto (1978) incorporated the classical Rudnicki and Rice (1975) strain localization criterion into the Gurson model for modeling void coalescence. It is known that the Rudnicki and Rice criterion works well for the cases with yield surface vertex and nonassociated flow rules. Thomason (1990) has shown that the prediction of the Gurson model with the Rudnicki and Rice criterion using associated flow rule does not yield realistic ductility predictions. Instead, Thomason proposed a plastic limit load model-based void coalescence mechanism. Thomason argues that void coalescence coincides with the occurrence of plastic limit load state of the void-matrix cell. For a given void-matrix geometry, a virtual critical axial stress inducing the plastic flow localized in the horizontal ligament between neighboring

voids can be calculated based on a plastic limit load analysis. The vertical critical stress is a function of the inter-void geometry and is decreasing with the increase of void volume fraction. The virtual localized deformation mode can be realized only when the applied maximum principal stress is larger than or equal to the virtual critical stress. Zhang and Niemi (1994, 1995) were the first to test the plastic limit load-based void coalescence criterion in the Gurson model. By comparing with the micromechanical finite element analysis results by Koplik and Needleman (1988), it has been found that that Thomason's plastic limit load coalescence model is fairly accurate for describing coalescence of nonhardening materials. By incorporating the Thomason plastic limit load coalescence mechanism into the Gurson model, a so-called complete Gurson model is obtained (Zhang et al., 2000). The advantage of the complete Gurson model is that ductile fracture is solely determined by the void nucleation parameter(s). It has been clearly indicated that the critical void volume fraction is not a material constant (Zhang and Niemi, 1994, 1995). The critical void volume fraction depends on void nucleation parameters, stress triaxiality, and plastic strain hardening. The void volume fraction at the end of coalescence has been shown to be relatively independent of the stress triaxiality and can be approximated by $f_F = 0.15 + 2f_0$, where f_0 is the initial void volume fraction (Zhang et al., 2000). Thomason's plastic limit load model has been further modified by Pardoen and Hutchinson (2000), considering hardening materials and void shape effect. The hardening effect was considered by Zhang et al. (2000). The void shape-induced anisotropy has also been studied by Benzerga et al. (2002). Theoretical and analytic microvoid coalescence models have been presented by Gologanu et al. (2001). Significant progress in micromechanics of void coalescence has recently been made by the Pardoen group (Lassance et al., 2006, 2007; Fabregue and Pardoen, 2008), including a new constitutive model developed for elastic–plastic materials, which contain both primary and secondary voids.

The unit cell model pioneered by Koplik and Needleman (1988), has been widely used to numerically investigate the void growth and coalescence behavior of periodically voided ductile materials and verify the analytical constitutive models (Brocks et al., 1995; Kuna and Sun, 1996). In almost all of these works, the unit cell was subjected to a proportional loading. The effect of uniaxial prestrain on ductile fracture has not been carefully studied. To the best knowledge of the authors, almost no study has been carried out so far on the effect of prestrain history on micro failure mechanisms, except a few studies on the cyclic plasticity effect on void growth (Ristinmaa, 1993). The authors are motivated by the recent industry drive in characterizing the prestrain effect (Wästberg et al., 2004). Understanding the effect of prestrain history on the micro failure mechanisms is an important step in studying the

tensile properties and fracture toughness of steels subjected to prestrain histories. The focus of this study will be put on the effect of uniaxial tensile prestrain on microvoid coalescence. It is hoped that the results of this study helps to understand the pipe-reeling-induced prestrain effect. A uniaxial tensile prestrain range up to 10% is considered.

Stress controlled axisymmetric unit cells with and without axial prestrain history are used to investigate the void coalescence. Void coalescence is commonly measured by the bifurcation point of the vertical strain–horizontal strain relation (Koplik and Needleman, 1988). In this study, it has been found that the microscopic position of the maximum axial stress in the inter-void matrix ligament is an indicator of void coalescence. Void coalescence starts when the position of the maximum axial stress appears at the cell model boundary. The effect of prestrain history on void coalescence can be illustrated by the equivalent strain needed to move the maximum axial stress from the void edge to the cell boundary. The prestrain effect can also be explained by the effect of prestrain-induced strain hardening and prestrain-induced void shape change.

In the following, the numerical procedure used in this study is described first. The void coalescence without a prestrain history is studied with focus on the stress distribution in the inter-void void ligament as well as void shape change. The effect of prestrain on void coalescence strain and explanation of the effects in terms of prestrain-induced strain hardening and void shape change are presented last and the article is closed with a summary and concluding remarks.

MATERIALS AND NUMERICAL PROCEDURE

The void matrix material is characterized by a model material. The yield stress of the virgin matrix material σ_0 is set to be 400 MPa. The elastic properties of the model material are taken as $E/\sigma_0 = 500$ and $\nu = 0.3$. In the present work, rate-independent power law strain hardening material was assumed. The flow stress of the virgin matrix material is described as:

$$\sigma_f = \sigma_0 \left(1 + \frac{\varepsilon_p}{\varepsilon_0}\right)^n \tag{1}$$

where σ_f is the flow stress, ε_p the equivalent plastic strain, σ_0 the yield stress, $\varepsilon_0 = \sigma_0/E$ the yield strain, and n the plastic strain hardening exponent. A moderate hardening exponent $n = 0.05$ has been used which is a good representation of the high strength pipeline steels used in the offshore industry.

Two prestrain cases, one with 5% and one with 10% have been considered. The prestrain here means the permanent strain after unloading.

Prestrain induces strain hardening and residual stress in the void model as well as void growth and void shape changes. In order to separate the strain hardening effect from the one due to void shape changes, ellipsoidal, and spherical voids with a void volume faction equivalent to the one at the end of prestrain history and a homogenous prestrained matrix material have been analyzed. Figure 1 compares the virgin material with the two homogenous prestrained matrix materials used in this study. The stress–strain curves of the materials with prestrain 5 and 10% shown in the figure were obtained by trimming the virgin material curve by the specified prestrain level. The elastic properties of the prestrained materials are kept identical to the virgin material.

Figure 2 shows the quarter unit cell model used in the study. The model has been used previously for studying the void coalescence behavior (Zhang et al., 2000). The model is axisymmetric and the stress ratios $\rho = \Sigma_x/\Sigma_y$ are
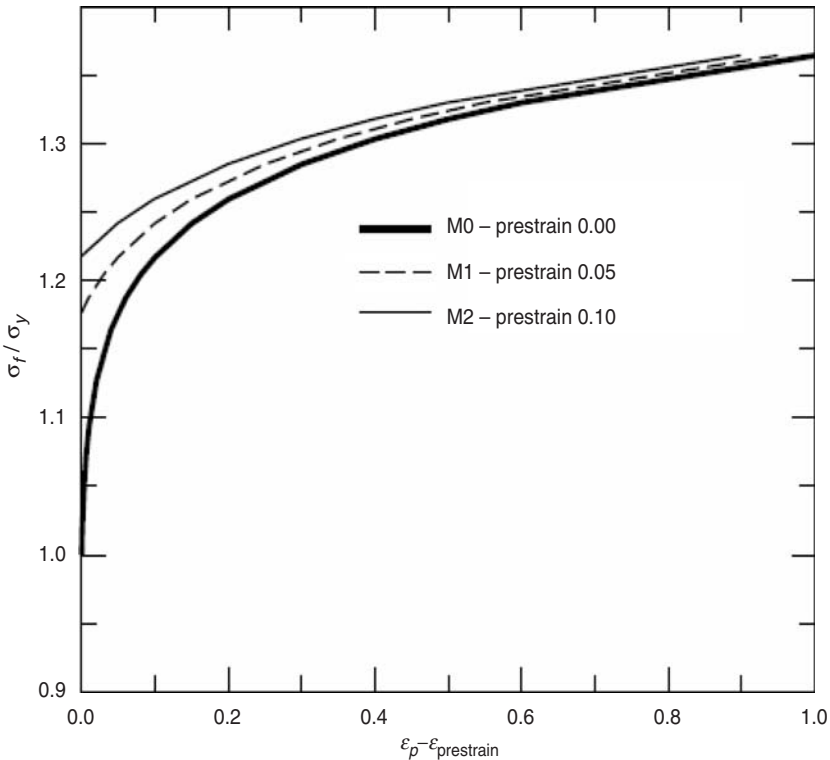
Figure 1. Matrix material properties used in the analyses. The yield stress for the virgin material (M0) is 400 MPa. The numbers in the legend indicate the uniaxial prestrain applied to the matrix material.
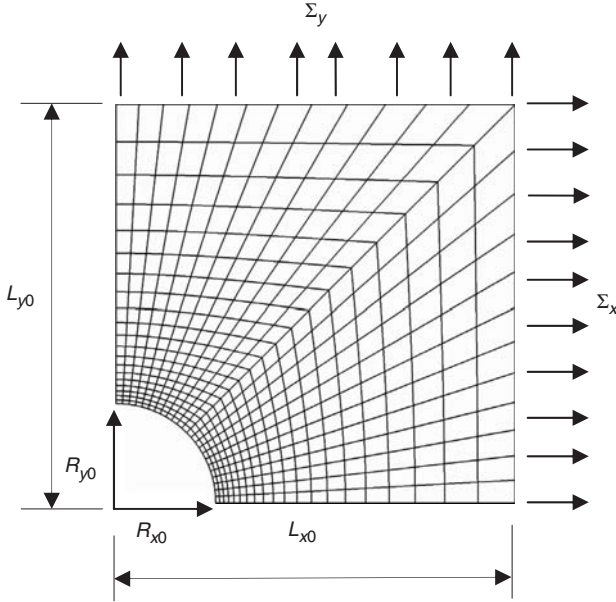
**Figure 2.** Finite element model used in the analyses.

kept constant in both the prestraining analysis and subsequent analyses. The model was analyzed in a load-controlled manner and ABAQUS RIKS method has been applied. Nodal constraints were applied such that the left and top boundaries remain vertical and horizontal during the analysis. For the axisymmetric problem considered the stress triaxiality can be calculated from the stress ratio ρ:

$$T = \frac{\sigma_h}{\sigma_{eq}} = \frac{1 + 2\rho}{3(1 - \rho)} \tag{2}$$

where σ_h is the hydrostatic stress and σ_{eq} the von Mises equivalent stress.

The initial radius and height of the model are denoted as L_{x0} and L_{y0}, and R_{x0} and R_{y0} represent the initial radii of the void. The results are based mainly on the case with an initial void volume fraction 1.04%. This void volume fraction has been used by Koplik and Needleman (1988) and Gologanu et al. (2001). Voids with different initial shapes (spherical, prolate, and oblate) but same initial void volume fraction are also considered, Figure 3. The initial and current void aspect ratios are defined as,

$$S_0 = \frac{R_{y0}}{R_{x0}}, \quad S = \frac{R_y}{R_x}. \tag{3}$$
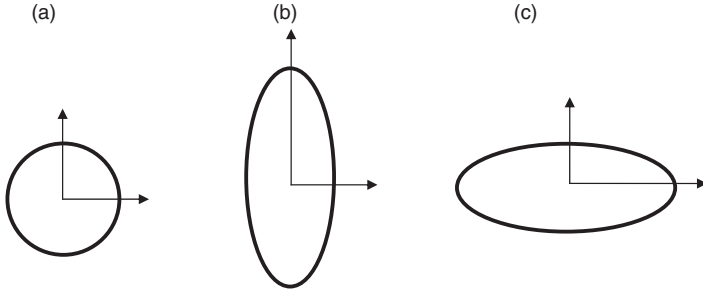
Figure 3. *Three initial void shapes considered in the study (a) spherical void with S = 1, (b) prolate void with S = 4, and (c) oblate void with S = 0.25.*

The mesoscopic principal strains and effective strain of the cell model are calculated according to:

$$E_x = \ln\left(\frac{L_x}{L_{x0}}\right); \quad E_y = \ln\left(\frac{L_y}{L_{y0}}\right); \quad E_e = \frac{2}{3}\left(E_y - E_x\right) \tag{4}$$

INTER-VOID STRESS DISTRIBUTIONS AND VOID COALESCENCE

We revisit the coalescence behavior of a typical cell model without prestrain history. In the work of Koplik and Needleman (1988), void coalescence is defined as the incident when the mesoscopic radial deformation (E_x) becomes constant – further deformation takes place in a uniaxial straining mode. Figure 4(a) shows the mesoscopic vertical strain versus radial strain curve for the case with stress triaxiality $T = 1.0$. The cell model elongates in the vertical direction and contracts in the radial direction. During the plastic deformation and void growth, an approximate linear relation can be observed. This linear relation indicates a homogenous deformation state. When the deformation reaches a critical state a sudden shift from the relatively homogenous deformation state to a uniaxial straining state ($\Delta E_x = 0$) can be seen. This shift depicts the onset of void coalescence.

The mesoscopic coalescence behavior of the cell model represented by Figure 4(a) is well understood. However, the microscopic explanation as why and when the coalescence occurs is unclear. It is interesting to understand what really happens microscopically inside the inter-void matrix when the void coalescence occurs. For this purpose, the axial stress distributions along the void ligament at different deformation levels are presented in Figure 4(b). In Figure 4(b), the abscissa represents the normalized ligament: $x = 0$ indicates the void edge and $x = 1.0$ implies the cell boundary.
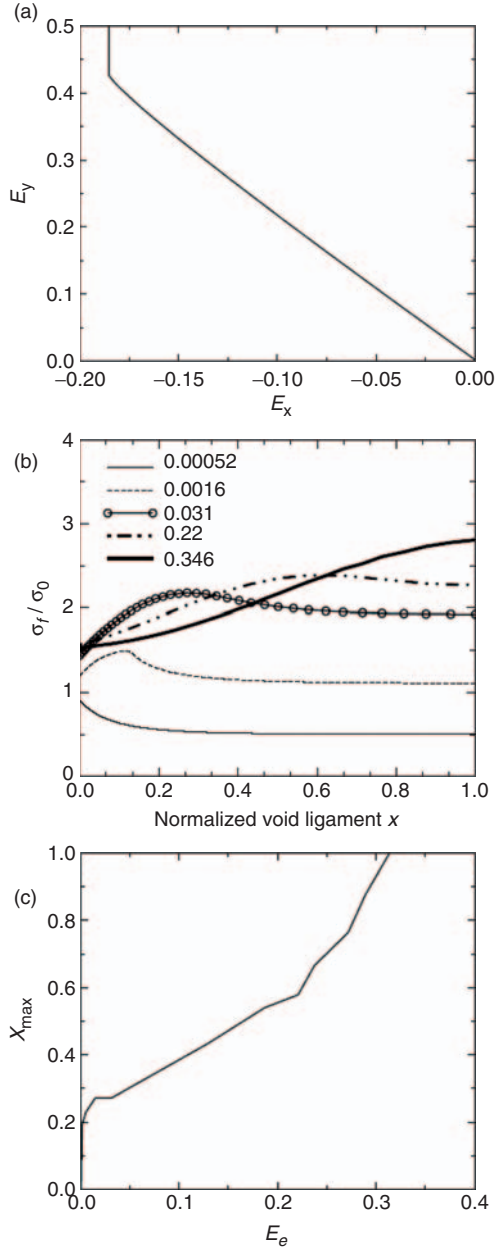
Figure 4. *Cell model behavior for the case with f = 1.04%, T = 1.0. (a) Axial versus radial deformation behavior, (b) axial stress distribution along the ligament, and (c) position of the peak axial stress in the inter-void ligament versus mesoscopic equivalent strain.*

The normalized axial stress (Σ_y/σ_0) is plotted in the ordinate. The number in the legend shows the mesoscopic equivalent strains and five levels have been shown.

It is obvious that because of the elastic stress concentration the peak axial stress occurs at the void edge ($x=0$) when the load is small and the cell is elastic. As the load increases, plastic deformation develops and the position of the maximum axial stress moves towards the cell boundary. The absolute value of the peak axial stress also increases with loading. At an equivalent strain about 32% the peak axial stress in the ligament occurs at the cell boundary ($x=1$). This stage corresponds to the starting of void coalescence and shifting from a relatively homogenous deformation state to a localized deformation mode. Please note that the equivalent strain at which the peak stress first time reaches at the cell boundary is slightly smaller than the value observed from the mesoscopic criterion using Figure 4(a). Further loading will not change the position of the peak axial stress in the ligament and the absolute value of the peak axial stress will start to decrease due to the global unloading of the cell model.

Plastic deformation in a cell model always starts at void edge ($x=0$) and the plastic region enlarges from the void edge outwards. Figure 4(b) shows that it is the plastic deformation in the ligament, which moves the peak axial stress toward the cell boundary. The cell model is stable when the surrounding material has sufficient constraint to hold the peak stress far away from the cell boundary. When a significant part of the cell model is plastic and no surrounding material can provide sufficient constraint to hold the peak axial stress, void coalescence then starts.

We may therefore take the position of the peak axial stress (x_{max}) in the normalized ligament as a microscopic coalescence indicator. Figure 4(c) plots the x_{max} as a function of the equivalent strain E_e. $x_{max}=0$ depicts that the cell model is elastic and $x_{max}=1$ indicates the starting of void coalescence. Figure 4(c) shows that when the equivalent strain is very small (less than 1%) the peak axial stress has already moved to a position 20% of the ligament from the void edge. The x_{max} in the range between 25% and 60% is approximately a linear function of E_e. x_{max} increases faster when it passes about 60%. The x_{max} versus equivalent strain diagram will also be used in the following to study the effect of prestrain history.

It should be noted that the findings in Figure 4(b) and (c) further support Thomason's plastic limit load theory for void coalescence (Thomason, 1990). Thomason argues that void coalescence coincides with a state where plastic limit load is reached and no further deformation in a homogenous mode is possible. When the peak axial stress has moved to the cell boundary, the plastic deformation is fully developed in the model and a plastic limit state has been reached.
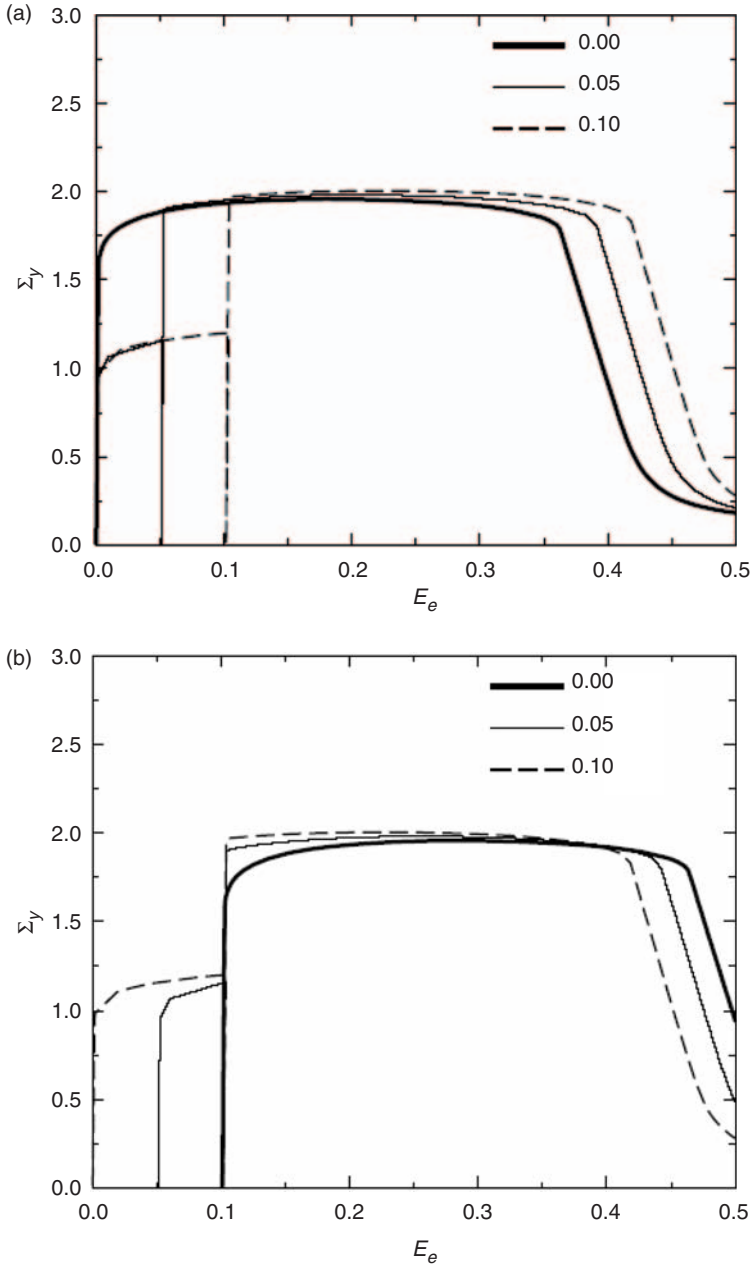
EFFECT OF PRESTRAIN ON VOID COALESCENCE

Prestrain Effect on Void Coalescence Strain

In this study, a 'low to high' stress triaxiality scenario is considered. A uniaxial loading ($T = 0.33$) is applied to the unit cell model up to a specified prestrain level before unloading. The model is then re-loaded with a constant stress ratio ρ (higher stress triaxiality) until void coalescence. The stress ratio ρ varies from 0.4, 0.5, 0.6 to 0.7 and the corresponding stress triaxiality are 1.0, 1.33, 1.83, and 2.67, respectively.

Figure 5(a) shows an example of mesoscopic axial stress versus equivalent strain curves. Here axial stress and equivalent strain are chosen, because both are relevant coalescence parameters. A spherical void with an initial void volume fraction 1.04% is analyzed. The uniaxial loading stopped at a prestrain 0.05 and 0.1, further loading with a higher stress triaxiality $T = 1.0$ continued until void coalescence. The effect of prestrain can be clearly seen in Figure 5(b), where the mesoscopic axial stress versus equivalent strain curves for the loading with $T = 1.0$ have been translated such that they have the same starting point in the loading range ($T = 1.0$). It can be observed from Figure 5(b) that the mesoscopic axial stress of the cell model becomes higher when a prestrain is applied. At the same time the mesoscopic equivalent strain at coalescence is reduced. In the following the reduction of the coalescence strain (ductility) will be the focus.

For the case without a prestrain history, the effect of initial void shape on void coalescence has been studied by many authors and is well understood (Pardoen and Huntchinson, 2000; Benzerga et al., 2002). It should be noted that the void shape is usually not a void coalescence criterion (it does not enter the coalescence criterion directly) and relative void spacing is probably a more interesting parameter. However, void shape is a physical parameter and easy to understand. For a given cell model geometry, the void shape and void spacing are interrelated. The general observation is that the mesoscopic coalescence strain is the largest when the initial void is prolate and smallest when the initial void is oblate. The effect of void shape on coalescence is more pronounced at low stress triaxiality and is decreasing with increasing stress triaxiality (Pardoen and Hutchinson, 2000). Figure 6 displays the coalescence strain (mesoscopic equivalent strain at coalescence determined by the Koplik and Needleman criterion) E_c versus stress triaxiality diagram for the three types of voids considered.

In general, prestrain has a negative effect on the coalescence strain. It is interesting to observe that both the stress triaxiality and void shape have a strong influence on the reduction of the coalescence strain. For a 10% prestrain history and initially spherical void the reduction in the coalescence

Figure 5. *Prestrain effect on load-carrying behavior (a) from undeformed state (b) translated curves. The stress triaxiality analyzed is 1.0.*
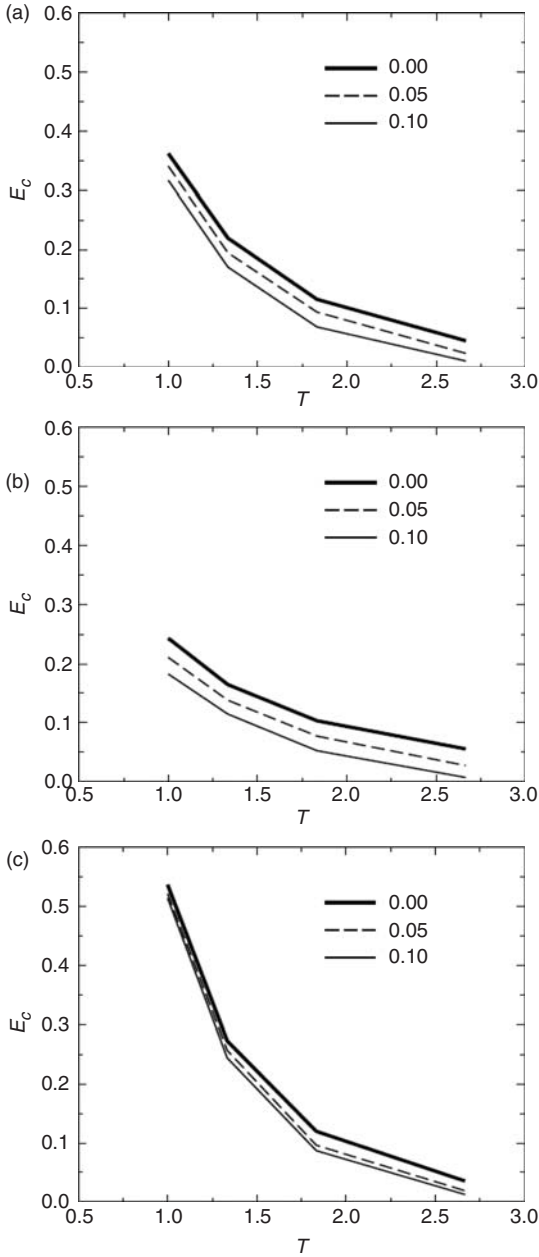
Figure 6. *Effect of prestrain on the void coalescence strain, (a) spherical void with S = 1, (b) oblate void with S = 0.25, and (c) prolate void with S = 4. The numbers in the legend indicate the prestrain levels.*

strain can be as large as 75% for the case with $T=2.67$. For the spherical void, it can be seen that the net reduction of the coalescence strain due to the prestrain history is slightly increased at high stress triaxiality. A stronger reduction in the coalescence strain can be seen for the oblate void, Figure 6(b). The net reduction is nearly constant and independent of stress triaxiality. The effect of prestrain on the coalescence strain for the prolate void is less significant compared with both the spherical and oblate voids. When the stress triaxiality is below 1.33, the prestrain effect can be neglected for the initially prolate void considered in the study.

The effect of prestrain history on the x_{max} versus E_e relation is shown in Figure 7 for the cases with stress triaxiality $T=1.0$ and 1.83. It can be seen that for a given equivalent strain the x_{max} is much larger for the case with prestrain history and than the one without. Consequently, a prestrain makes the peak ligament stress reach the boundary much quicker than the case without a prestrain history, leading to a significant reduction in ductility.

During a prestrain history, plastic deformation occurs in the void ligament. Upon unloading a self-balanced residual stress field will be built up in the cell model. In addition, the prestrain history will also induce void growth and void shape change. In the following the effect of void geometry change (void growth and shape change) and prestrain-induced residual stress and hardening will be studied separately.
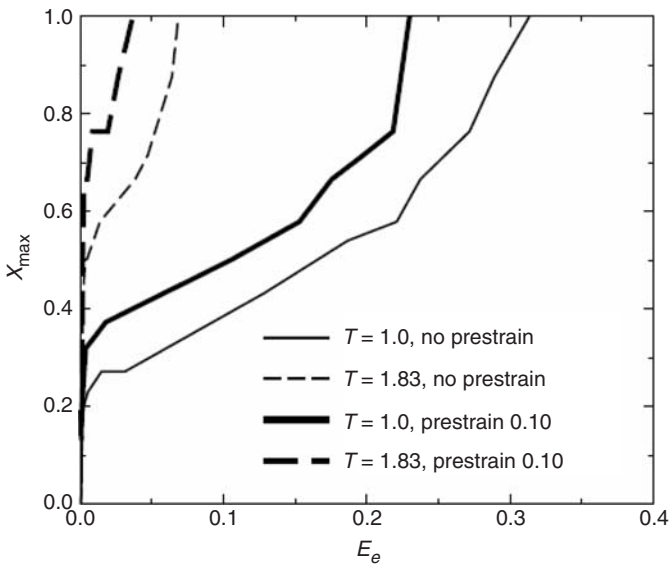

Figure 7. *Effect of prestrain on the position of peak tensile stress in the void ligament.*

Prestrain-induced Local Strain Hardening and Residual Stress Distribution

Figure 8(a) shows the distribution of the flow stresses along the ligament of an initially spherical void after a prestrain of 5 and 10%, respectively. Due to the void, stress concentration occurs and it will lead to plastic
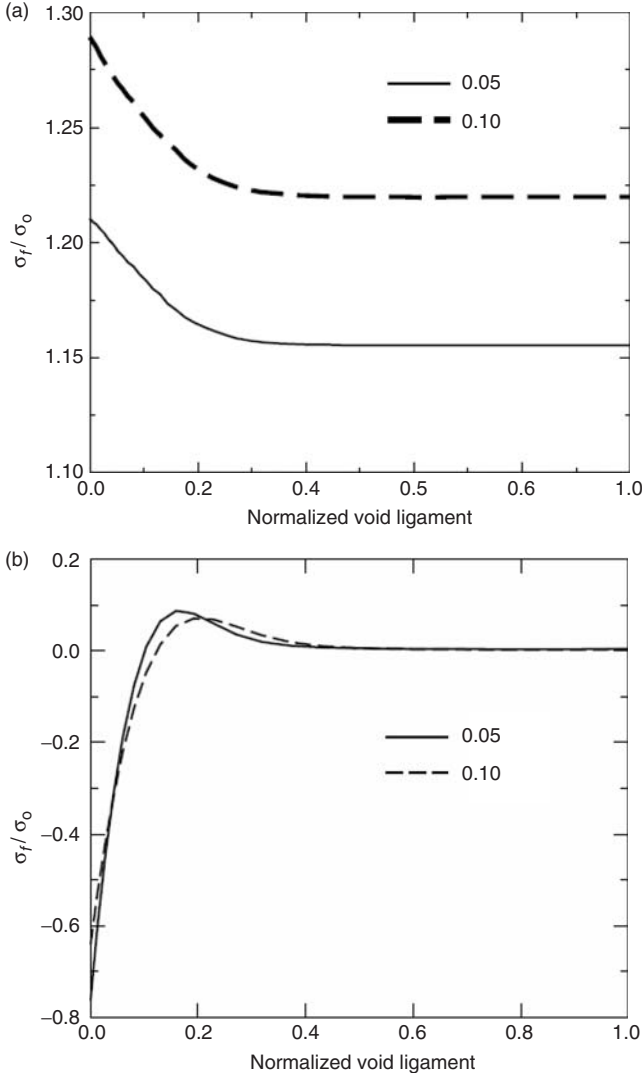

Figure 8. (a) Prestrain-induced strain hardening and (b) residual axial stress distributions along the void ligament at load-free condition. The initial void volume fraction is $f_0 = 1.04\%$.

deformation first at the area close to void edge. The maximum flow stresses were elevated to 1.22 and 1.27 times of the yield stress for the two prestrain levels considered.

The residual stress (axial stress) distributions of the two prestrain history cases after unloading are shown in Figure 8(b). A compressive residual stress up to 60–80% of the initial yield stress can be seen. A peak axial residual stress occurred at about 18–20% of the ligament. It can be observed that the residual stress distribution is only weakly dependent on the prestrain history.

Prestrain-induced Void Shape Change

For a void with an initial void volume fraction 1.04% the void volume fractions at the end of 5 and 10% prestrain history are 1.12 and 1.18%, respectively. The absolute void growth is small and effect of the void growth during the prestrain history on the later coalescence behavior is therefore insignificant. In the following we will focus on the effect of void shape change. Figure 9 shows the void shape change of an initially spherical void during a prestrain loading and subsequent reloading with different stress triaxiality. For a 10% prestrain the void aspect ratio of a spherical void increases about 35%. For the case with $T=1.0$ the void aspect ratio
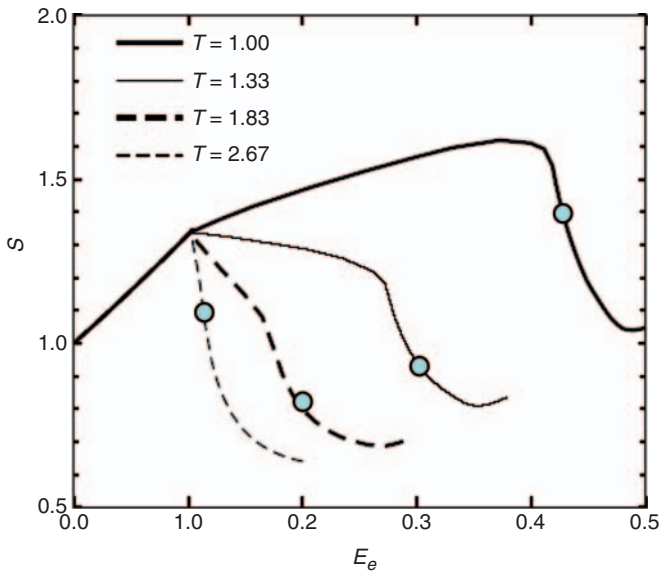

Figure 9. *Void shape change during the transition from low stress triaxiality prestrain loading to higher stress triaxiality loadings with a prestrain 10%. In the figure the solid point indicates the strarting point of void coalescence.*

continues to increase while for higher stress triaxiality the void aspect ratio starts to decrease.

The effect of prestrain history on the void shape change at constant stress triaxiality 1.33 is displayed in Figure 10. From the literature it is well known that in the case without prestrain history the void aspect ratio increases with the plastic deformation and an initially spherical void will thus become prolate. However, for the same spherical void with a 10% prestrain history the void aspect ratio during the reloading decreases with the increase of plastic deformation. When the spherical void was subjected to a 5% prestrain history the void aspect ratio increased to 1.18. For this prestrain, it is interesting to note that the void aspect ratio during subsequent reloading with stress triaxiality 1.33 will stay approximately constant.

Effect of Strain Hardening versus Effect of Void Shape Change

Both local strain hardening and void shape change induced by the prestrain history influence void coalescence. It is difficult to separate the effect of residual stress from the effect of strain hardening. In the following the combined effect of strain hardening and residual stress will be called strain-hardening effect. In order to isolate the local strain hardening effect from the void shape change effect, equivalent ellipsoidal void with the same
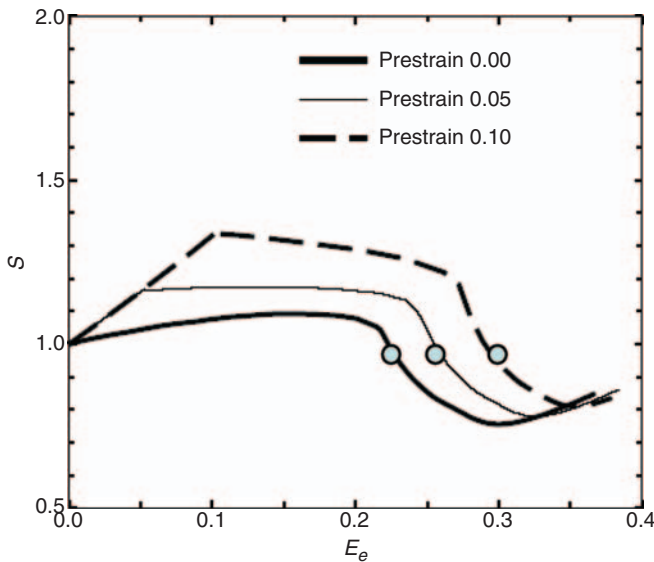
Figure 10. Effect of prestrain levels on void shape change for $f_0 = 1.04\%$ and $T = 1.33$. In the figure the solid point indicates the starting point of void coalescence.

void aspect ratio and same void volume fraction as the prestrained void in the beginning of high stress triaxiality loading has been analyzed using a homogenously prestrained matrix material. The yield stress for the homogenously prestrained material was obtained by truncating the original true stress-strain curve by the same amount of prestrain, Figure 1, where M1 and M2 represent the homogenous matrix materials with prestrain 5 and 10%, respectively. These materials used represent the mesoscopic behavior. In order to further study the effect of void shape change on void coalescence, equivalent spherical void with same void volume fraction as the prestrained void in the beginning of high stress triaxiality loading, and with the same homogenous material has also been analyzed.
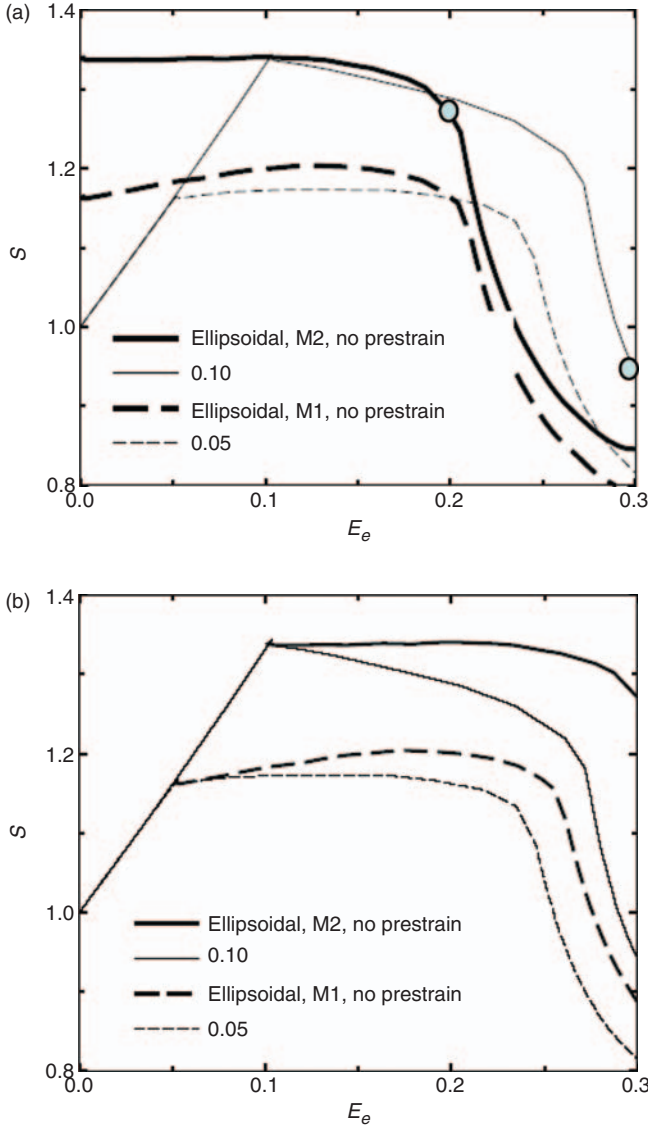
Figure 11(a) compares the void aspect ratio versus equivalent strain relation of the ellipsoidal voids with that of the prestrained voids with an initial spherical shape. The results of ellipsoidal voids in Figure 11(a) have been translated by the amount of prestrain in the *x*-axis in Figure 11(b) to have the same starting point as the results of prestrained voids. Results in Figure 11(b) show that for the same geometrically identical voids the void aspect ratio of the one with prestrain strain history decreases faster than that of the one with homogenous material. It must be noted that the void coalescence strain will also be reduced. Figure 11 clearly shows that the strain hardening in the cell model due to the prestrain history plays a significant role.

Finally the contributions of strain hardening and void shape change on the reduction of coalescence strain are illustrated in Figure 12. In Figure 12, 'M0, no prestrain' represents the case without a prestrain history, 'M0, prestrain 0.10' denotes the result of the case with a 10% prestrain history. Figure 12 shows that the effect due to void shape change is relatively small while the effect of prestrain-induced strain hardening before the loading with high stress triaxiality is significant. This observation is same for cases both with low and high stress triaxiality.

SUMMARY AND CONCLUDING REMARKS

Void coalescence is the last stage of ductile failure mechanism. Mesoscopically, onset of void coalescence corresponds to the instant where a relatively homogenous deformation localizes to the horizontal intervoid ligament. Further deformation occurs in the axial direction and the size of the ligament keeps constant. The onset of coalescence of a void cell model can be numerically detected from the mesoscopic radial strain versus axial strain curve. Once the coalescence starts a sharp vertex can be seen in the mesoscopic radial strain versus axial strain curve.

The results in this study show that the onset of coalescence can also be explained microscopically. Due to the void geometry and stress

Figure 11. *Void aspect ratio versus mesoscopic strain for the case with T = 1.33.*

concentration the peak axial stress in the intervoid ligament occurs at the void edge when the mesoscopic loading is small and the cell model is dominated by elastic deformation. The position of peak axial stress moves gradually toward the cell boundary with the increase of plastic deformation.
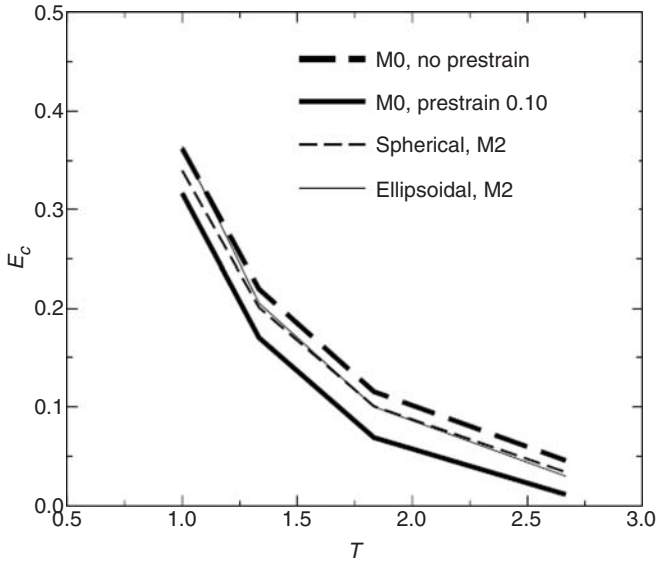
Figure 12. *Effect of void shape change and residual stress on the void coalescence for the case with $f_0 = 1.04\%$ and prestrain 0.10.*

Finally, when the peak axial stress appears at the outer boundary the void coalescence starts. The microscopic coalescence criterion is not practical and has not been applied to determine the coalescence strain. However, this observation further verifies the plastic limit load theory for void coalescence by Thomason. Void coalescence occurs when a plastic limit load state of the void cell model has been reached.

The effect of plastic prestrain on the void coalescence behavior is strongly dependent on the stress triaxiality and the initial void shape. For prolate voids with stress triaxiality smaller than 1.5, the prestrain effect can be neglected. At high stress triaxiality cases the reduction in coalescence strain due to the prestrain history can be very significant. For an initially spherical void with $T = 2.67$ the reduction in coalescence strain can be as large as 75% for a 10% prestrain. For prolate voids with initial void aspect ratio 4 and initial void volume fraction 1.04% the effect of prestrain up to 10% on coalescence strain can be neglected when the stress triaxiality is less or equal to 1.3. In comparison, the effect of prestrain on the coalescence strain of oblate voids is the largest. For the oblate void with initial void aspect ratio 0.25 more than 20% reduction has been observed for the case with stress triaxiality $T = 1$. The absolute reduction of coalescence strain seems to be constant and independent of stress triaxiality. As can be expected, the reduction of coalescence strain of spherical voids is somewhat between the

two extreme cases analyzed. It must be noted that the coalescence strain meant here is the coalescence strain in the re-loading step with higher stress triaxiality. The sum of the total strain (applied prestrain + coalescence strain) indeed increases with the increase of the prestrain.

Plastic prestrain history induces both strain hardening and void shape changes. Calculations with ellipsoidal void and homogenous prestrained matrix material truncated by the amount of the prestrain show that the prestrain-induced strain hardening plays the major role in reducing the coalescence strain. The effect of void shape change during the plastic prestrain on the coalescence is relatively small.

In this study the effect of prestrain on the coalescence of a pre-existing void is the focus. The present study follows the pioneering work by Koplik and Needleman where a cell model with an existing void in the middle was used. It should be noted that the prestrain effect on void coalescence alone may not completely account for the observed reduction in fracture toughness (Fukuda et al., 2005). Engineering steels contain both large inclusions and particles, which nucleate voids in the beginning of plastic loading and small secondary particles that can nucleate voids during the plastic deformation. The true ductility of a material consists of two parts – the strain to void nucleation and the strain from void nucleation to coalescence. Only the last part has been studied here. Recently, studies by Gao and Kim (2006) have shown that voids nucleated from the secondary particles during the plastic deformation can have a significant effect on the coalescence. The larger the prestrain the more voids nucleated, and the more reduction in ductility.

Fukuda et al. (2005) has shown that both compressive and tensile prestrain will contribute to the reduction of fracture toughness. A void does not grow in a compressive prestrain history. In the case with compressive history, it must be the void nucleation, which reduces the toughness. The analysis of compressive prestrain involves cyclic plasticity effect of kinematic hardening behavior and will be the focus of further studies. It has been demonstrated that Thomason' coalescence criterion is very accurate for both hardening and nonhardening matrix materials. It is not clear whether Thomason's model is still working in the cases with prestrain history. Further work will also include the verification of Thomason's criterion for prestrain cases.

REFERENCES

Benzerga, A.A., Besson, J., Batisse, R. and Pineau, A. (2002). Synergistic Effects of Plastic Anisotropy and Void Coalescence on Fracture Mode in Plane Strain, *Modelling and Simulation in Materials Science and Engineering*, **10**: 73-102.

Brocks, W., Sun, D.Z. and Honig, A. (1995). Verifications of the Transferability of Micromechanical Parameters by Cell Model Calculations with Visco-plastic Materials, *International Journal of Plasticity*, **11**: 971–989.

Chae, D., Bandstra, J.P. and Koss, D.A. (2000). The Effect of Prestrain and Strain-path Changes on Ducile Fracture: Experimental and Computational Modelling, *Materials Science and Engineering* A, **285**: 165–171.

Cosham, A. (2001). A Model of Prestrain Effects on Fracture Toughness, *Journal of Offshore Mechanics and Arctic Engineering*, **123**: 182–190.

Enami, K. (2005). The Effects of Compressive and Tensile Prestrain on Ductile Fracture Initiation in Steels, *Engineering Fracture Mechanics*, **72**: 1089–1105.

Fabrègue, D. and Pardoen, T. (2008). A Constitutive Model for Elastoplastic Solids Containing Primary and Secondary Voids, *Journal of the Mechanics and Physics of Solids*, **56**: 719–741.

Fukuda, N., Hagiwara, N. and Masuda, T. (2005). Effect of Prestrain on Tensile and Fracture Properties of Line Pipes, *Journal of Offshore Mechanics and Artic Engineering*, **127**: 263–268.

Gao, X. and Kim, J. (2006). Modeling of Ductile Fracture: Significance of Void Coalescence, *International Journal of Solids and Structures* **43**: 6277–6293.

Garrison, W.M. and Moody, N.R. (1987). Ductile Fracture, *Journal of Physics and Chemistry of Solids*, **48**: 1035–1047.

Gologanu, M, Leblond, J.-P. Perrin, G. and Devaux, J (2001). Theoretical Models for Void Coalescence in Porous Ductile Solids, I. Coalescence "in Layers", *International Journal of Solids and Structures*, **38**: 5581–5594.

Gurson, A.L. (1975). Plastic Flow and Fracture Behaviour of Ductile Materials Incorporating Void Nucleation, Growth And Coalescence, PhD Dissertation, Brown University.

Koplik, J. and Needleman (1988). A. Void Growth And Coalescence in Porous Plastic Solids. *International Journal of Solids and Structures*, **24**, 835–853.

Kuna, M. and Sun, D.Z. (1996). Three Dimensional Cell Model Analysis of Void Growth in Ductile Materials, *International Journal of Fracture*, **81**: 235–258.

Lassance, D., Scheyvaerts, F. and Pardoen, T. (2006). Growth and coalescence of penny-shaped voids in metallic alloys, *Engineering Fracture Mechanics*, **73**: 1009–1034.

Lassance, D., Fabre'gue, D., Delannay, F. and Pardoen, T. (2007). Micromechanics of Room and High Temperature Fracture in 6xxx Al Alloys, *Progress in Materials Science*, **52**: 62–129.

Martinez, M. and Brown, G. (2005). Evolution of Pipe Properties during Reel-lay Process: Experimental Characterisation and Finite Element Modelling, In: *Proceedings of the 24th International Conference on Offshore Mechanics and Arctic Engineering (OMAE 2005)*, June 12–17, Halkidiki, Greece.

Needleman, A. and Tvergaard, V. (1992). Analysis of Plastic Flow Localization in Metals, *Applied Mechanics Review*, **45**: s3–s18.

Pardoen, T. and Hutchinson, J.W. (2000). An Extended Model for Void Growth and Coalescence, *Journal of the Mechanics and Physics of Solids*, **48**: 2467–2512.

Qiu, H., Enoki, M., Hiraoka, K. and Kishi, T. (2005). Effect of Prestrain on Fracture Toughness of Ductile Structural Steels under Static and Dynamic Loading, *Engineering Fracture Mechanics*, **72**: 1624–1633.

Ristinmaa, M. (1993). Cyclic Plasticity and its Numerical Treatment, PhD Thesis, Lund University.

Rudnicki, J.W. and Rice, J. (1975). Conditions for the Localization of Deformation in Pressure-sensitive Dilatant Materials, *Journal of the Mechanics and Physics of the Solids*, **23**: 371–394.

Sivaprasad, S., Tarafder, S., Ranganath, V.R., Ray, K.K. (2000). Effect of Prestrain on Fracture Toughness of HSLA Steels, *Material Science and Engineering A*, **284**: 195–201.

Thomason, P.F. (1990). *Ductile Fracture of Metals*, Pergamon Press, Oxford.

Tvergaard, V. (1981). Influence of Voids on Shear Band Instabilities under Plane Strain Conditions, *International Journal of Fracture*, **17**: 389–407

Tvergaard, V. (1982). On Localization in Ductile Materials Containing Voids, *International Journal of Fracture* **18**: 237–251.

Wästberg, S., Pisarski, H. and Nyhus, B. (2004). Guidelines for Engineering Critical Assessments for Pipeline Installation Methods Introducing Cyclic Plastic Strain, In: *23rd International Conference on Offshore Mechanics and Arctic Engineering*, June 20–25, Vancouver, British Columbia, Canada, OMAE2004–51061.

Yamamoto, H. (1978). Conditions for Shear Localization in the Ductile Fracture of Void-containing Materials, *International Journal of Fracture*, **14**: 347–365.

Zhang, Z.L. and Niemi, E. (1995). A New Failure Criterion for the Gurson-Tvergaard Dilatational Constitutive Model, *International Journal of Fracture*, **70**: 321–334.

Zhang, Z.L. and Niemi, E. (1994). Analyzing Ductile Fracture by Using Dual Dilatational Constitutive Equations. *Fatigue & Fracture of Engineering Materials and Structures*, **17**: 695–707.

Zhang, Z.L., Thaulow, C. and Ødegård, J. (2000). A Complete Gurson Model Based Approach for Ductile Fracture, *Engineering Fracture Mechanics*, **67**: 155–168.